# Chapter – 3

## *Molecular dynamics simulation study of adsorption of endocrine disruptive chemicals (EDCs) on $NiFe_2O_4$ surface.*

## 3.1 Introduction

Phenols are high-priority environmental pollutants due to their toxicity and potential for environmental accumulation[152]. Adsorption is widely regarded as an effective method for wastewater treatment owing to its high efficiency, selectivity, cost-effectiveness, and significant adsorption capacity[153,154]. The limited adsorption capacity and challenging separation processes associated with conventional adsorbents demand the development of advanced materials with superior adsorption performance, facile separation, and low operational costs.

Recent studies have highlighted the crucial role of $NiFe_2O_4$-based magnetic nano adsorbents in removing organic and inorganic pollutants from aqueous solutions[82,155]. Experimental reports have demonstrated the adsorption of phenol and bisphenol A (BPA) on nickel ferrite nanoparticles [156,157]. For instance, L. Mohammadi et al. experimentally investigated the adsorption behavior of phenol on $NiFe_2O_4$ nanocomposites and further analyzed it using an artificial neural network model[156]. The experimental adsorption data fitted the Langmuir isotherm model, indicating the monolayer adsorption. On the other hand, Di et al. synthesized the covalent organic framework and $NiFe_2O_4$-based nanocomposite to selectively capture BPA from various actual water samples[157]. These authors also employed molecular dynamics simulation to investigate the interaction of bisphenol A with the covalent organic framework part of the adsorbent[157]. Nevertheless, the authors did not investigate the contribution of the $NiFe_2O_4$ part of the composite to the adsorption of BPA from an aqueous medium. Thus, the atomic-level mechanisms underlying the adsorption of phenol and BPA on the nickel ferrite component in composites remain poorly understood. A comprehensive understanding of the mechanism can facilitate the modification of the adsorbent surface, optimizing it for targeted wastewater

remediation. A detailed computational study can provide valuable insights into the adsorption mechanism.

Given the lack of adsorption research from this perspective, this chapter investigates the adsorption mechanism of BPA and phenol on the $NiFe_2O_4$ surface through classical MD simulations in an aqueous medium. The present investigation addresses how these organic molecules interact with the $NiFe_2O_4$ (311) surface in the presence of water molecules. The density profile data was used to determine the adsorption isotherms followed in each case. The molecular interactions between the $NiFe_2O_4$ surface and these organic molecules are studied using radial distribution function data.

## 3.2 Methodology

### 3.2.1 Computational methodology

The Materials and Process Simulation (MAPS) program (published by SCIENOMICS) version 4.1.1 was utilized for molecular modelling [143]. Molecular dynamics (MD) simulations were utilized using the Large-Scale Atomic/Molecular Massively Parallel Simulator (LAMMPS) program. The modified Dreiding force field was applied to model interactions [134]. The Van der Waal component of the Dreiding force field is provided by the function below in equation (3.1).

$$E_{lj}^{LJ} = 4\varepsilon_0 \left[ \left( \frac{\sigma_0}{r_{ij}} \right)^{12} - \left( \frac{\sigma_0}{r_{ij}} \right)^{6} \right] \qquad (3.1)$$

The function mentioned in equation (3.1) denotes the well depth as $\varepsilon_0$, van der Waal radii as $\sigma_0$, and the distance between atom types i and j as $r_{ij}$. The 12-6 Lennard Jones (LJ) interaction parameters were obtained from the Dreiding force field database [134]. Table 3.1 provides details of these interaction parameters. The Lorentz–Berthelot combination rules

were applied to describe the mixed non-bonded interactions between $NiFe_2O_4$, solute, and water atoms.

**Table 3.1** LJ 12-6 Potential Parameters used in MD simulations.

| Atom type | $\epsilon_0$ (kcal/mol) | $\sigma_0$(Å) |
|---|---|---|
| Ni (Nickel of $NiFe_2O_4$) | 0.015 | 2.834 |
| Fe (Iron of $NiFe_2O_4$) | 0.055 | 4.540 |
| O_3 (Lattice oxygen of $NiFe_2O_4$) | 0.0957 | 3.4046 |
| O_2 (Oxygen attached to the ring carbon of phenol and BPA) | 0.0957 | 3.4046 |
| H__HB (Hydrogen attached to the phenolic oxygen of phenol and BPA) | 0.0001 | 3.195 |
| H_ (Hydrogen attached to the ring carbon of phenol and BPA) | 0.0152 | 3.195 |
| C_R (Ring carbon of phenol and BPA) | 0.0951 | 3.8983 |
| C_3 (Methyl carbon of BPA) | 0.0951 | 3.8983 |
| H_W (Hydrogen of water) | 0.0 | 0.0 |
| O_W (Oxygen of water) | 0.102 | 3.188 |

### 3.2.2 Model building and computational setup

The XRD pattern of $NiFe_2O_4$ shows that the (311) plane has the highest intensity[82]. Given this, adsorption studies of phenol and BPA on $NiFe_2O_4$ were conducted on its (311) surface[82]. A parallelepiped simulation cell with dimensions of 35.98 Å × 34.96 Å × 35 Å was constructed for this purpose. Then, a $NiFe_2O_4$ slab of dimension 35.98 Å × 34.96 Å × 7.00 Å was placed in the middle of the simulation cell such that it was perpendicular to the z-axis of the simulation box (Figure 3.1a). The geometries of phenol and BPA were modelled (Figure 3.1b-d) and optimized by the MNDO (Modified Neglect of Diatomic Overlap) method [158]. Water molecules were modelled as per the TIP3P model (Table 3.2)[142].

Equal numbers of solute or adsorbate (phenol or BPA) and TIP3P water molecules (at fixed density ~1.1 g/cc) were inserted into the space on both sides of the $NiFe_2O_4$ (311) slab by the amorphous builder tool (Figure 3.2a and 3.2b) of MAPS molecular modelling software. Different simulation systems were built to investigate the adsorption of 12, 14, 16, 18, 20, 22, and 24 molecules of phenol and 4, 6, 8, 10, 12, 14, and 16 BPA molecules in 1500 molecules of TIP3P water.

**Table 3.2** TIP3P water model parameters.

| **Parameter** | **Value** |
|---|---|
| O_W-H_W bond ($k_b$ , $r_0$) | 450 Kcal/mol/Å$^2$, 0.9572 Å |
| H_W-O_W-H_W ($k_a$ , θ) | 55 Kcal/mol, 104.52˚ |
| O_W charge | -0.834 |
| H_W charge | 0.417 |

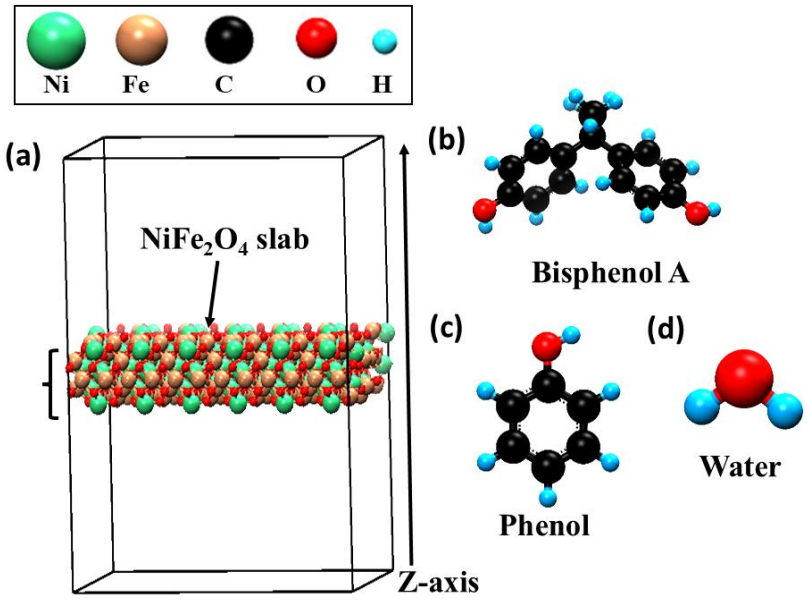


**Figure 3.1** (a) Simulation box containing $NiFe_2O_4$ (311) slab in the middle. Optimized structures of (b) bisphenol A, (c) phenol, (d) water molecule.

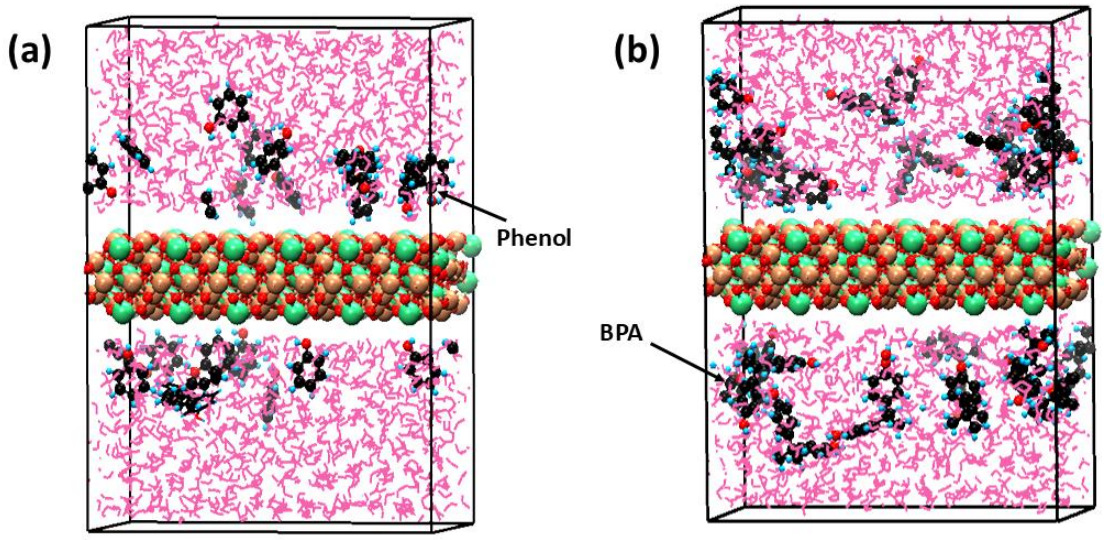


**Figure 3.2** Image (a) shows the initial configuration of a simulation run, with the simulation box containing 24 phenol and 1500 water molecules. Figure (b) displays the initial configuration of a simulation box containing 16 BPA molecules with 1500 TIP3P water molecules. (Note- The solute (phenol or BPA) and water molecules are divided equally on both sides of the $NiFe_2O_4$ (311) slab in the simulation box.)

Each system was subjected to an NVT MD simulation run for 10 nanoseconds (hereafter denoted by ns) and a time step of 1 femtosecond (hereafter denoted by fs). The cut-off for nonbonded interactions was 12 Å, with the particle mesh approach used to calculate Coulomb interactions. In all simulations, the temperature was fixed at 298.15 K. The atoms constituting the $NiFe_2O_4$ (311) surface were fixed throughout the simulation. Results shown here use the time-averaged data obtained from a three-nanosecond production run at the end of the trajectories.

## 3.3 Result and Discussions

### 3.3.1 Adsorption studies

Figures 3.3a and 3.3b depict the system at the beginning and end of the ten-nanosecond molecular dynamics (MD) simulation, illustrating the initial presence of phenol molecules

and their final configuration. Almost all phenol molecules are adsorbed on the $NiFe_2O_4$ (311) surface after 10 ns. Similarly, Figures 3.4a and 3.4b show the snapshots of an initial system containing BPA molecules at the start and the final system at the end of the ten-nanosecond MD simulation run. All the BPA molecules moved towards the nickel ferrite slab from both sides and got adsorbed after the simulation run. By observing the simulation box more closely, it is observed that some of the phenol and BPA molecules interact with the $NiFe_2O_4$ (311) surface in such a manner that the plane of the phenyl ring in phenol and BPA is parallel to the $NiFe_2O_4$ surface.

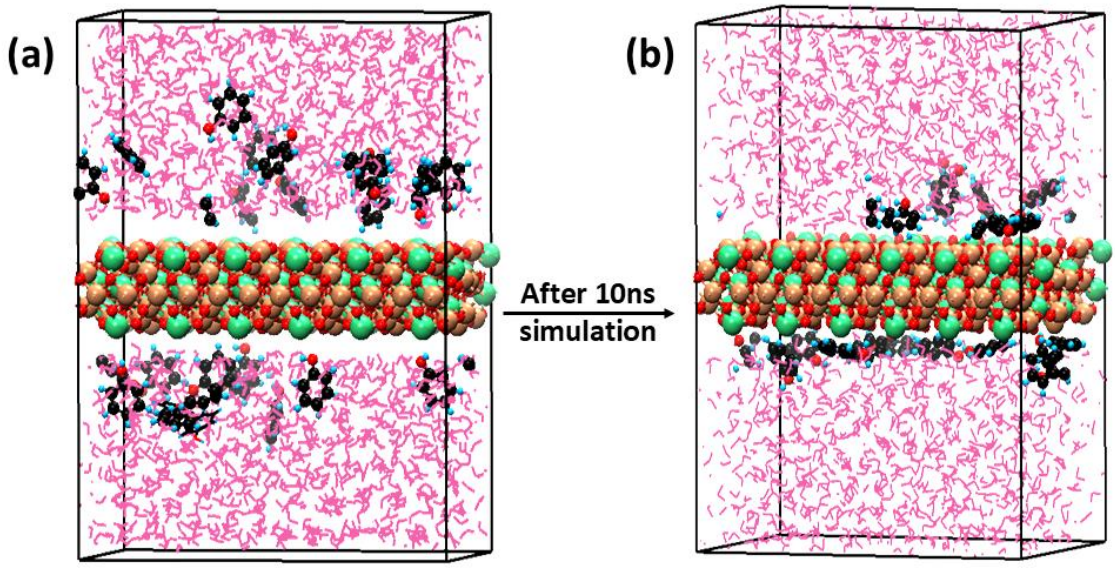


**Figure 3.3** The snapshots of the simulation box containing $NiFe_2O_4$ (311) surface are surrounded by 24 phenols and 1500 TIP3P water molecules. (a) At the start and (b) at the end of the simulation.

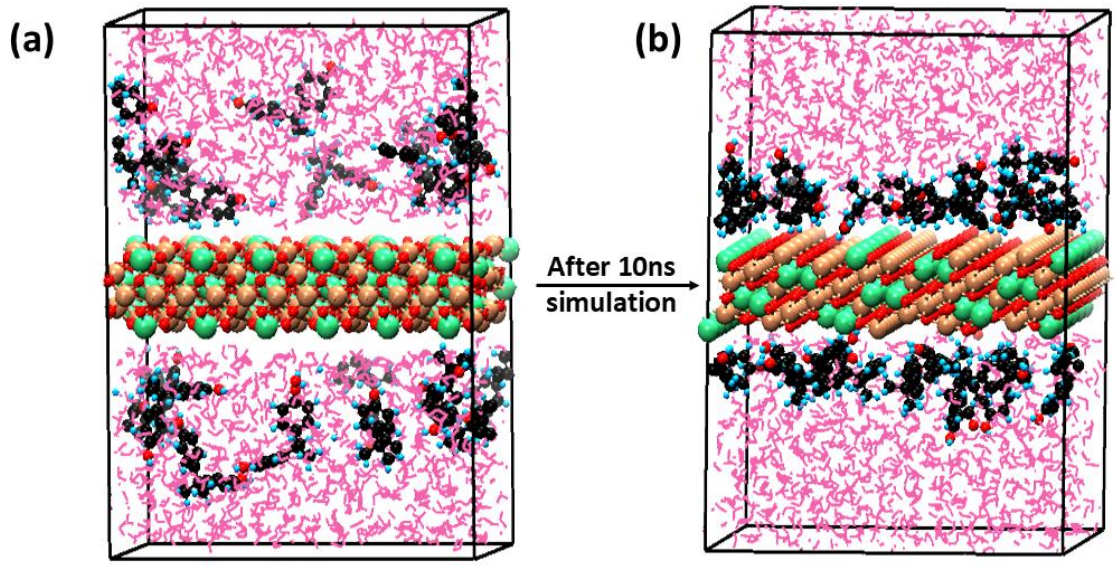


**Figure 3.4** Snapshots of simulation box containing $NiFe_2O_4$ (311) surface surrounded by 16 BPA, and 1500 TIP3P water molecules (a) at the start and (b) at the end of the simulation.

### 3.3.2 Density Profile Analysis

Figures 3.5a and 3.5b represent the density profiles plotted of solute molecules with distance along the z-axis of the simulation box for systems containing four different concentrations of phenol (12,18, 22, and 24) and BPA (4, 8, 14, and 16) molecules, respectively. The black peak in the middle denotes the $NiFe_2O_4$ (311) slab. The area under a peak gives the adsorbate molecules in that layer over the adsorbent surface. The first peak of density plots on either side of the $NiFe_2O_4$ (black) peak denotes the first adsorbed layer over the $NiFe_2O_4$ (311) adsorbent surface. Figures 3.5a and 3.5b show that the density of the adsorbed molecule is proportional to the initial concentration of the adsorbate molecule. The density of adsorbed phenol molecules increases with the concentration of phenol molecules, specially from 12 to 22 phenol molecules. Likewise, the adsorbed BPA molecule concentration also increases with the respective solute concentration, specially from 4 to 14 BPA molecules. At higher concentrations, however, the density profiles exhibit a tendency toward saturation, as the peak intensity no longer increases significantly. This

behavior indicates that the active sites on the $NiFe_2O_4$ surface progressively become occupied.

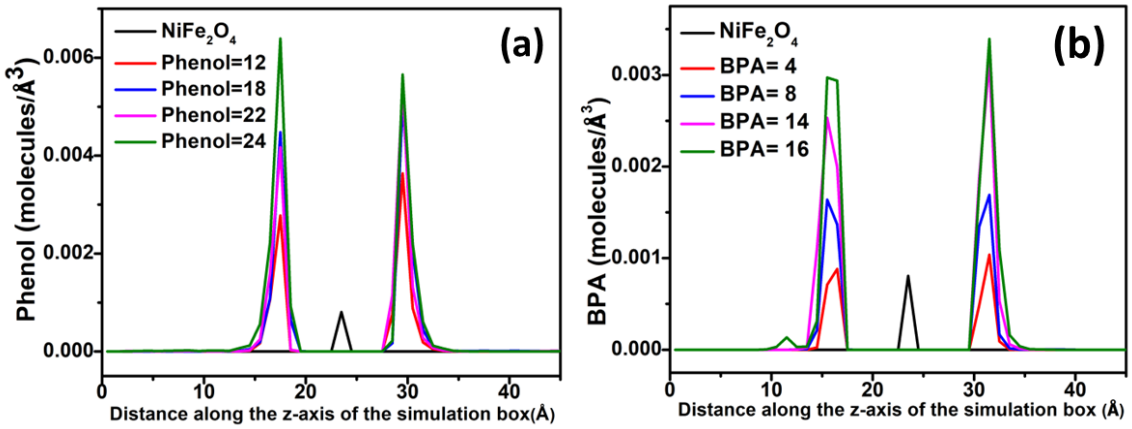


**Figure 3.5** The time-averaged density profile plots for (a) phenol and (b) BPA adsorption on $NiFe_2O_4$ (311) surface.

### 3.3.3 Adsorption isotherm

The adsorption isotherm describes the equilibrium distribution of adsorbate molecules on the surface of an adsorbent. It defines the relationship between the concentration of adsorbate on the adsorbent surface and its concentration in the surrounding liquid phase. The number of unbound adsorbate molecules reflects the amount of free solute remaining in solution. [159]. For each initial solute concentration, the number of adsorbed molecules is quantified by integrating the area under the first peak of the corresponding density profile. The obtained adsorption data were fitted to the non-linear equations of Langmuir, Freundlich, and Langmuir-Freundlich adsorption isotherm models in terms of the number of adsorbed and unbound (or free) adsorbate molecules [113,159]. Equations 3.2, 3.3, and 3.4 are the nonlinear equations of the Langmuir, Freundlich, and Langmuir-Freundlich (LF) adsorption isotherm models, respectively. These equations are expressed in terms of the

number of solute molecules adsorbed to the adsorbent surface and the number of unbound solute molecules.

$$N_{ads} = \frac{k_l N_{free}}{1+k_l N_{free}} \quad (3.2)$$

$$N_{ads} = k_f N_{free}^{1/n} \quad (3.3)$$

$$N_{ads} = \frac{K\, N_{free}^{1/n}}{1+k N_{free}^{1/n}} \quad (3.4)$$

In equation 3.2, 3.3, and 3.4, $\boldsymbol{N_{ads}}$ represents the number of adsorbate molecules adsorbed to the $NiFe_2O_4$ surface ($N_{bound}$), $\boldsymbol{N_{free}}$ represents the number of free adsorbate molecules, $\boldsymbol{k_l}, \boldsymbol{k_f}, and\ \boldsymbol{K}$ denote equilibrium constants for Langmuir, Freundlich, and Langmuir-Freundlich adsorption isotherms, $\boldsymbol{n}$ signifies the heterogeneity factor ($\boldsymbol{n}$ >1).

**Table 3.3** The isotherm fitting parameters for the MD adsorption data of phenol and BPA.

| **Adsorbate** | **Langmuir-Freundlich isotherm** | | | **Freundlich isotherm** | | | **Langmuir isotherm** | |
|---|---|---|---|---|---|---|---|---|
| | ***K*** | ***n*** | **$R^2$** | $k_f$ | ***N*** | **$R^2$** | $k_l$ | **$R^2$** |
| Phenol | 2.894 | 2.005 | 0.995 | 8.694 | 1.30 | 0.923 | 3.068 | 0.986 |
| BPA | 1.011 | 1.569 | 0.994 | 11.281 | 2.678 | 0.991 | 4.460 | 0.958 |

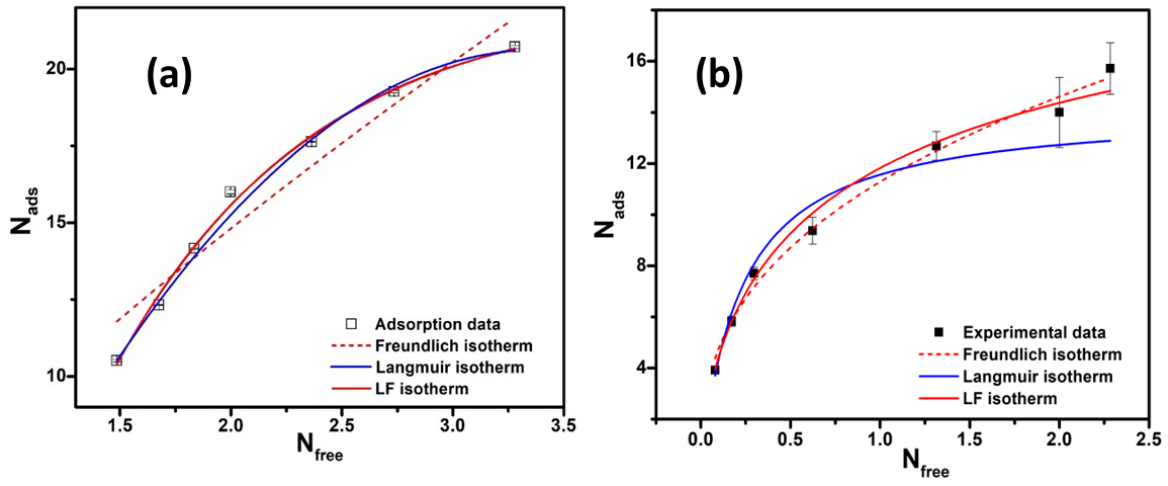


**Figure 3.6** Nonlinear adsorption isotherms fit for (a) Phenol and (b) BPA adsorption on $NiFe_2O_4$ (311) surface.

Table 3.3 shows the adsorption isotherm parameters for computed adsorption data for phenol and BPA adsorption. Figure 3.6a shows that the adsorption data obtained from the MD simulations for phenol fits poorly with the Freundlich isotherm model. In contrast, the phenol adsorption simulation data fits Langmuir and Langmuir-Freundlich isotherms well. This result also agrees with the experimental result obtained by L. Mohammadi et al. because their adsorption data fits the Langmuir isotherm at higher phenol concentrations [156]. Notably, these authors only fitted their experimental isotherm data to Langmuir and Freundlich equations. The present MD simulation data predicts that the best fit should be obtained with the Langmuir-Freundlich isotherm equation ($0.994<R^2<0.995$) (Figure 3.6b).

MD simulation data shows that BPA adsorption to the $NiFe_2O_4$ (311) surface follows the Freundlich and Langmuir-Freundlich models almost equally well. The correlation coefficients for the fits to these models are almost the same. Note that there is no experimental report on the adsorption of BPA in aqueous medium on $NiFe_2O_4$ particles. The order of isotherm constant values of LF isotherm for phenol and BPA is $k_{BPA} > k_{phenol}$.

Thus, the MD simulation data predicts that BPA molecules should be more strongly adsorbed on the $NiFe_2O_4$ particles than phenol molecules.

### 3.3.4 Radial Distribution Function (RDF) analysis

Adsorbate-adsorbent interactions can only be distinguished by long-time averaged RDF graphs between distinct atom types. A radial distribution function (RDF) plot depicts the probability of an atom type occurring near another atom type. The RDF plots in Figures 3.7a and 3.7b describe the dominant interactions between constituent atoms of the phenol (24 molecules), BPA (16 molecules), and the $NiFe_2O_4$ (311) surface, respectively. Only the first peak in each RDF plot between two different atom types is considered for analysis because it represents the closest interaction distance between the considered atom types.

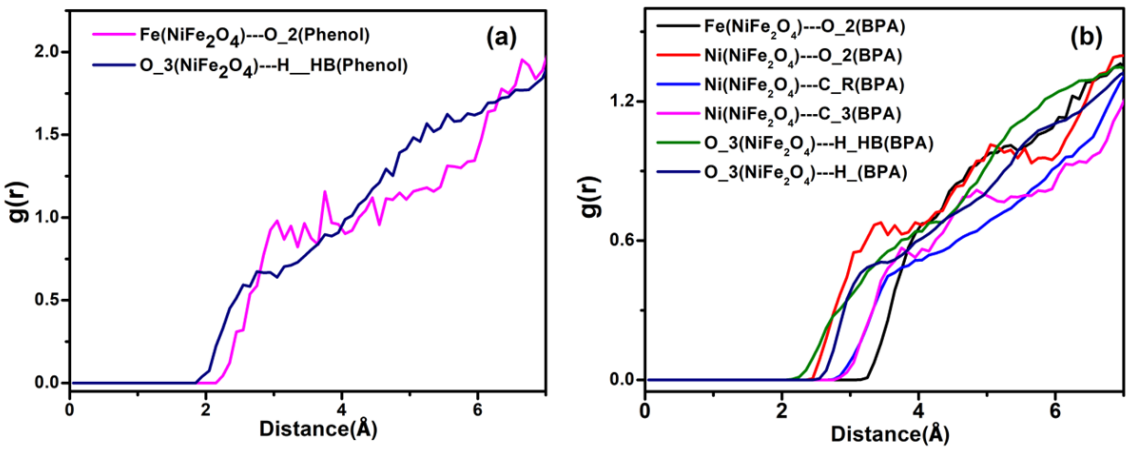


**Figure 3.7**. The radial distribution function g(r) between different atom types of (a) phenol and (b) BPA with those on the $NiFe_2O_4$ (311) surface. [Abbreviations for different atom type- Ni: Nickel of $NiFe_2O_4$, Fe: Iron of $NiFe_2O_4$, O_3: Lattice oxygen of $NiFe_2O_4$, O_2: Oxygen attached to the ring carbon of the phenol and BPA, H__HB: Hydrogen bonded to the phenolic oxygen of phenol and BPA, H_: Hydrogen bonded to the ring carbon of phenol and BPA, C_R: Ring carbon of phenol and BPA, C_3: methyl carbon of BPA, r: represents the distance of approach in Å]

These measurements indicate the probability of finding the considered atom type at that distance. The first interaction peaks in these plots represent the most significant nonbonded interaction dominating the proceedings. In Figure 3.7a, the navy-blue peak at ~2.4Å shows the interaction of lattice oxygens of $NiFe_2O_4$ (O_3) with hydrogen atoms of hydroxyl groups (H__HB) in phenol molecules. This interaction distance fulfils the criteria of hydrogen bond formation [160]. At ~2.8Å, the pink curve shows another interaction between the Fe of $NiFe_2O_4$ (Fe) and the phenol molecule's oxygen atom (O_2). This interaction complements the first interaction between O_3 and H__HB atom types. The electrostatic attraction between Fe ($NiFe_2O_4$)-O (phenol) strengthens the hydrogen bonding phenomenon [161].

In Figure 3.7b, the first olive color peak at ~2.4 Å shows a strong interaction between lattice oxygen (O_3) of $NiFe_2O_4$ and a hydroxyl hydrogen atom (H__HB) of the BPA molecule. This indicates the formation of hydrogen bonding between BPA and $NiFe_2O_4$ surface. The red peak at ~2.6 Å, having the highest g(r) value, represents the electrostatic interaction of the Ni atom of $NiFe_2O_4$ with the hydroxyl oxygen atom of BPA molecules[161]. The interactions represented by the olive green and red curves are the main adsorption interactions between BPA and the $NiFe_2O_4$ surface. Interactions other than these, like the navy-blue peak at ~2.6Å due to the interaction between the $NiFe_2O_4$ lattice oxygen and the ring hydrogen atom of BPA molecules, complement the first two interactions. Moreover, this navy-blue peak is less intense than the red peak. Further, royal blue and pink peaks are at almost the same distance, ~3.0 Å, indicating the interaction of nickel atoms of $NiFe_2O_4$ with ring carbon and the methyl carbon atom of BPA, respectively. The previous interaction could be due to a weak cation-$\pi$ interaction between Ni ($NiFe_2O_4$) – carbon ring of BPA molecules [162]. At ~3.2Å, the first peak of the black RDF plot appears. It is due to a complementary interaction between a lattice Fe atom of the $NiFe_2O_4$ surface and the oxygen

atom of BPA. Therefore, electrostatic attraction and hydrogen bond formation dominate over other intermolecular interactions between phenol- $NiFe_2O_4$ and BPA- $NiFe_2O_4$.

## 3.4 Conclusions

Molecular dynamics simulations were conducted to investigate the adsorption mechanisms of phenol and BPA from aqueous solutions onto the (311) surface of $NiFe_2O_4$. The simulations were performed for $NiFe_2O_4$ systems with varying concentrations of both phenol and BPA. Analysis of the resulting density profiles revealed that phenol adsorption closely follows the Langmuir-Freundlich isotherms. In contrast, BPA adsorption exhibited a strong correlation with the Langmuir-Freundlich models. Moreover, the MD results suggest that BPA molecules exhibit a stronger affinity for the $NiFe_2O_4$ surface compared to phenol, indicating a higher adsorption strength. The long-time averaged radial distribution function of different adsorbate–adsorbent atomic interactions was analysed to clarify the adsorption mechanism. The RDF analysis revealed that phenol primarily adsorbs onto the $NiFe_2O_4$ (311) surface through hydrogen bonding between the lattice oxygen (O_3) of $NiFe_2O_4$ and the hydrogen atom of the hydroxyl group (H_HB) in the phenol molecule. Similarly, BPA exhibits strong interaction with $NiFe_2O_4$ via the same lattice oxygen (O_3) and the hydroxyl hydrogen (H_HB) of the BPA molecule. Overall, the combined results from RDF and isotherm analyses suggest that the $NiFe_2O_4$ (311) surface exhibits a heterogeneous nature, as both phenol and BPA interact with specific active sites on the surface.